Dual fermion approach to nonlocal correlations in the Hubbard model

A. N. Rubtsov,[1] M. I. Katsnelson,[2] and A. I. Lichtenstein[3]
[1]*Department of Physics, Moscow State University, 119992 Moscow, Russia*
[2]*Institute for Molecules and Materials, Radboud University, 6525 ED Nijmegen, The Netherlands*
[3]*Institute of Theoretical Physics, University of Hamburg, 20355 Hamburg, Germany*
(Received 26 October 2007; published 11 January 2008)

A diagrammatic technique is developed to describe nonlocal effects (e.g., pseudogap formation) in the Hubbard-like models. In contrast to cluster approaches, this method utilizes an exact transition to the dual set of variables, and it therefore becomes possible to treat the irreducible vertices of an effective *single-impurity* problem as small parameters. This provides a very efficient interpolation between weak coupling (band) and atomic limits. The antiferromagnetic pseudogap formation in the Hubbard model is correctly reproduced by just the lowest-order diagrams.

DOI: 10.1103/PhysRevB.77.033101 PACS number(s): 71.10.Fd, 05.30.Fk, 71.27.+a

Lattice fermion models with a strong local interaction (Hubbard-like models[1]) are believed to catch the basic physics of various systems, such as high-temperature superconductors,[2,3] itinerant-electron magnets,[4] Mott insulators,[5] ultracold atoms in optical lattices,[6] etc. Unfortunately, the analytical treatment of these problems is essentially restricted by the lack of explicit small parameters for the most physically interesting interactions. Direct numerical methods, such as exact diagonalization[7] or quantum Monte Carlo (QMC),[8,9] are limited by the clusters being of a relatively small size, or face other obstacles such as the famous sign problem for QMC simulations at low temperature.[10] There is a very successful approximate way to treat these models via the framework of so-called dynamical mean-field theory (DMFT),[5] where the lattice many-body problem is replaced with an effective impurity model. This approach is essentially based on the assumption of a local (i.e., momentum independent) fermionic self-energy. Indeed, there are numerous interesting phenomena which are basically determined by *local* electron correlations, such as Kondo effect,[11] Mott-Hubbard transitions,[5] and local moment formation in itinerant-electron magnets.[12] At the same time, momentum dependence of the self-energy is of crucial importance for Luttinger liquid formation in low-dimensional systems,[3,13] d-wave pairing in high-T_c superconductors,[2,14,15] and non-Fermi-liquid behavior due to van Hove singularities in two dimensions.[16] Recently, a rather strong momentum dependence of the effective mass renormalization in photoemission spectra of iron was observed.[17]

Currently, nonlocal many-body effects in strongly correlated systems are mainly studied via the framework of various cluster generalizations of DMFT.[14,15,18,19] Cluster methods do catch the basic physics of d-wave pairing and antiferromagnetism in high-T_c superconductors[14,15] and the effects of intersite Coulomb interaction in various transition-metal oxides.[20–22] At the same time, however, effects like Luttinger liquid formation or van Hove singularities cannot be described in cluster approaches. In such cases, the correlations are essentially long ranged and it is more natural to describe the correlations in momentum space. Recently, attempts have been made to consider nonlocal correlation effects in momentum space starting from DMFT as a zeroth-order approximation.[23,24] This approach requires a solution of ladder-like integral equation for complete vertex Γ and the subsequent use of the Bethe-Salpeter equation to obtain Green's functions. The first step here exploits an irreducible vertex of the effective impurity problem $\gamma^{(4)}$, whereas the second step uses just the bare interaction parameter U. This second step makes the generalized DMFT approach mostly suitable to the weak-coupling regime.[25]

In this Brief Report, we present a scheme which is accurate in both small-U and large-U limits and does not require numerically expensive solutions of any integral equations. A comparison of the results with lattice QMC simulations for the two-dimensional (2D) Hubbard model in the pseudogap regime demonstrates that the scheme is actually accurate even in the less-favorable case of intermediate U.

We proceed with a 2D Hubbard model with the corresponding imaginary-time action

$$S[c,c^*] = \sum_{\omega k\sigma} (\epsilon_k - \mu - i\omega) c^*_{\omega k\sigma} c_{\omega k\sigma} + U \sum_i \int_0^\beta n_{i\uparrow\tau} n_{i\downarrow\tau} d\tau. \tag{1}$$

Here, β and μ are the inverse temperature and chemical potential, respectively, $\omega=(2j+1)\pi/\beta, j=0,\pm1,\ldots$, are the Matsubara frequencies, and $\sigma=\uparrow,\downarrow$ is the spin projection. The bare dispersion law is $\epsilon_k=-2t(\cos k_x+\cos k_y)$, c^* and c are the Grassmannian variables, and $n_{i\sigma\tau}=c^*_{i\sigma\tau}c_{i\sigma\tau}$, where the indices i and k label sites and quasimomenta.

In the spirit of DMFT, we introduce a single-site reference system (an effective impurity model) with the action

$$S_{imp} = \sum_{\omega,\sigma} (\Delta_\omega - \mu - i\omega) c^*_{\omega,\sigma} c_{\omega,\sigma} + U \int_0^\beta n_{\uparrow\tau} n_{\downarrow\tau} d\tau, \tag{2}$$

where Δ_ω is as yet an undefined hybridization function describing the interaction of the effective impurity with a bath. We suppose that all properties of the impurity problem are known, so that its single-particle Green's function g_w is known, and the irreducible vertex parts $\gamma^{(4)}, \gamma^{(6)}$, etc. Our goal is to express the Green's function $G_{\omega k}$ and vertices Γ of the lattice problem in Eq. (1) via these quantities.

Since Δ is independent of k, the action (1) can be represented in the form

$$S[c,c^*] = \sum_i S_{imp}[c_i, c_i^*] - \sum_{\omega k\sigma} (\Delta_\omega - \epsilon_k) c^*_{\omega k\sigma} c_{\omega k\sigma}. \quad (3)$$

We utilize a dual transformation to the set of new Grassmannian variables f and f^*. The following identity:

$$e^{A^2 c^*_{\omega k\sigma} c_{\omega k\sigma}} = B^{-2} \int e^{-AB(c^*_{\omega k\sigma} f_{\omega k\sigma} + f^*_{\omega k\sigma} c_{\omega k\sigma}) - B^2 f^*_{\omega k\sigma} f_{\omega k\sigma}} df^*_{\omega k\sigma} df_{\omega k\sigma} \quad (4)$$

is valid for arbitrary complex numbers A and B. We chose $A^2=(\Delta_\omega-\epsilon_k)$ and $B^2=g_\omega^{-2}(\Delta_\omega-\epsilon_k)^{-1}$ for each set of indices ω, k, and σ.

With this identity, the partition function of the lattice problem $Z=\int e^{-S[c,c^*]} \mathcal{D}c^* \mathcal{D}c$ can be presented in a form $Z = Z_f \int\int e^{-S[c,c^*,f,f^*]} \mathcal{D}f^* Df \mathcal{D}c^* \mathcal{D}c$, where

$$S[c,c^*,f,f^*] = \sum_i S_{imp}[c_i, c_i^*] + \sum_{\omega k\sigma} [g_\omega^{-1}(f^*_{\omega k\sigma} c_{\omega k\sigma} + c^*_{\omega k\sigma} f_{\omega k\sigma}) + g_\omega^{-2}(\Delta_\omega - \epsilon_k)^{-1} f^*_{\omega k\sigma} f_{\omega k\sigma}] \quad (5)$$

and Z_f is a product $\Pi_{\omega k} g_\omega^2 (\Delta_\omega - \epsilon_k)$.

As a next step, we establish an exact relation between the Green's function of the initial system $G_{\tau-\tau',i-i'} = -\langle T c_{\tau i} c^*_{\tau' i'} \rangle$ and that of the dual system $G^{dual}_{\tau-\tau',i-i'} = -\langle T f_{\tau i} f^*_{\tau' i'} \rangle$. To this aim, we can replace $\epsilon_k \to \epsilon_k + \delta\epsilon_{\omega k}$ with a differentiation of the partition function with respect to $\delta\epsilon_{\omega k}$. Since we have two expressions for the action (1) and (5), one obtains

$$G_{\omega,k} = g_\omega^{-2} (\Delta_\omega - \epsilon_k)^{-2} G^{dual}_{\omega,k} + (\Delta_\omega - \epsilon_k)^{-1}, \quad (6)$$

where the last term follows from the differentiation of Z_f.

The crucial point is that the integration over the initial variables c_i^* and c_i can be performed separately for each lattice site, since $\Sigma_k (f_k^* c_k + c_k^* f_k) = \Sigma_i (f_i^* c_i + c_i^* f_i)$. For a given site i, one should integrate out c_i^* and c_i from the action that is equal to $S_{site}[c_i, c_i^*, f_i, f_i^*] = S_{imp}[c_i, c_i^*] + \Sigma_\omega g_\omega^{-1} (f^*_\omega c_\omega + c^*_\omega f_\omega)$. We obtain

$$\int e^{-S_{site}} \mathcal{D}c_i^* \mathcal{D}c_i = Z_{imp} \exp\left(- \sum_{\omega\sigma} g_\omega^{-1} f^*_{\omega i\sigma} f_{\omega i\sigma} - V[f_i, f_i^*] \right), \quad (7)$$

where Z_{imp} is a partition function of the impurity problem (2). The Taylor series for $V[f_i, f_i^*]$ in powers of f_i and f_i^* starts from $-\gamma^{(4)}_{1234} f^*_1 f_2 f^*_3 f_4$ (indices stand for a combination of σ and ω, for example, f_1^* means $f^*_{\sigma_1,\omega_1}$). Further Taylor series terms yield similar combinations including $\gamma^{(n)}$ of higher orders.

We arrive with an action S depending on the new variables f and f^* only:

$$S[f,f^*] = \sum_{\omega k\sigma} g_\omega^{-2} [(\Delta_\omega - \epsilon_k)^{-1} + g_\omega] f^*_{\omega k\sigma} f_{\omega k\sigma} + \sum_i V_i, \quad (8)$$

with $V_i \equiv V[f_i^*, f_i]$. In this dual action, the interaction terms remain localized in space, but are nonlocal in imaginary time, since, for example, $\gamma^{(4)}$ depends on the three independent Matsubara frequencies. To obtain the dual potential V for a practical calculation, one should solve then the impurity problem (2).

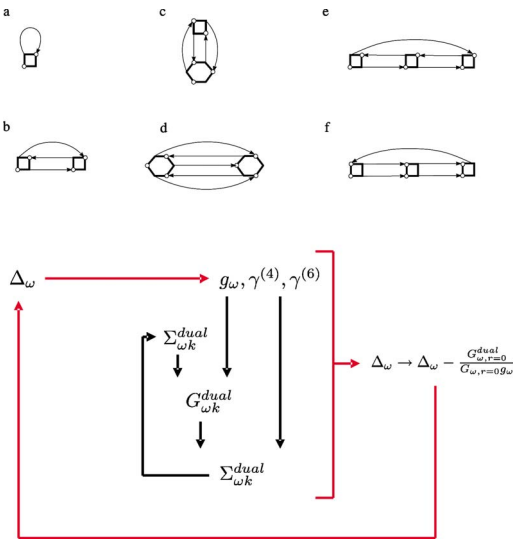

FIG. 1. (Color online) Various diagrams for Σ^{dual} and the scheme of calculation. The calculation includes "big" and "small" loops. The small loop is to determine the renormalized dual Green's function G^{dual} in a self-consistent way, for a given Δ, g, and $\gamma^{(n)}$. The big loop is to determine Δ. Only the big loop requires a solution of the impurity problem.

Finally, a regular diagrammatic expansion in powers of V can be performed. We draw skeleton diagrams, so that the lines in diagrams are renormalized dual Green's function, whereas the vertices are $\gamma^{(n)}$. The rules of diagram construction are very similar to usual ones, but the six-leg and higher-order vertices appear because $\gamma^{(6)}$ and higher terms are present in the series for V. Figure 1 shows several diagrams contributing dual self-energy $\Sigma^{dual}_{\omega,k} = -[(\Delta_\omega - \epsilon_k)^{-1} g_\omega^{-2} + g_\omega^{-1} + (G^{dual}_{\omega,k})^{-1}]$.

We use the skeleton-diagram expansion for the dual self-energy since it leads to the conserving theories, exactly like in conventional diagram technique.[26–28] The Baym criterion of a conservative theory is the existence of a functional of the Green function $\Phi[G]$ such that $\frac{\delta\Phi}{\delta G} = \Sigma$. Here, the variation δG comes from the infinitesimal variation of the Gaussian part of the action, $\delta (G^0)^{-1} c^* c$. In our consideration, we consider also the infinitesimal variations of the dual potential $\delta (G^0_{dual})^{-1} c^* c$. One can call an approximation dually Φ derivable if there exists a functional $\Phi^{dual}[G^{dual}]$ such as $\frac{\delta\Phi^{dual}}{\delta G^{dual}} = \Sigma^{dual}$, where the variation comes from $\delta (G^0_{dual})^{-1}$. Now, it turns out that the theory is Φ derivable if it is dually Φ derivable. The proof uses the relation between functional Φ and the partition function $\ln Z = \Phi - \mathrm{Tr}\, \Sigma G - \mathrm{Tr} \ln(-G) + C$ [here, C is an additive constant; see Eq. (47) of Ref. 27]. Since a similar relation takes place for Φ^{dual} and $\ln Z$, and since the partition function is the same for the initial and dual variables, this gives a one-to-one correspondence between $\Phi[G]$ and $\Phi^{dual}[G^{dual}]$.

It is important to understand what can be a small parameter in the expansion in dual diagrams. Clearly, if U is small,

then $\gamma^{(4)} \propto U, \gamma^{(6)} \propto U^2$, etc., and in the weakly correlated regime, vertices in the diagrams will be small (Fig. 1), and higher-order vertices will be even smaller.

At this point, we establish a condition for Δ, which was so far an arbitrary quantity. We use a self-consistent condition

$$\sum_k G^{dual}_{\omega,k} = 0. \tag{9}$$

It means that the simple closed loops in the diagrams vanish. In particular, this leads to the vanishing of the first-order "Hartree" corrections in the diagrammatic expansion. The diagram series of this kind has several important peculiarities. First of all, let us consider the zeroth-order approximation, $\Sigma^{(dual)}=0$. In this case, condition (9) becomes

$$\sum_k \frac{1}{g_\omega + (\Delta_\omega - \epsilon_k)^{-1}} = 0. \tag{10}$$

It is easy to show that this is exactly equivalent to the DMFT equation for the "hybridization function" Δ_ω.[5] It is known that DMFT behaves correctly near the atomic limit. In terms of the dual variables, one can observe that since $\epsilon, \Delta \ll g^{-1}$ near the atomic limit, it follows from condition (10) that $G^{dual} \approx g_\omega^2 \epsilon_k \ll g_\omega$ in this case. It is easy to check that this argumentation is valid for the scheme of an arbitrary diagrammatic order: the dispersion of G^{dual} is small near the atomic limit and, therefore, Eq. (9) means that lines in dual diagrams carry a small factor ϵg^{-1}. This ensures the fast convergence of a new diagrammatic expansion in the strong-coupling limit.

It should be noted that although Eq. (8) is formally similar to Eq. (1), analytical properties of G^{dual} differ from those of G. For example, since dual fermions are much more delocalized in time domain than the original one, $G^{dual}_{\omega\to\infty} \propto \omega^{-2}$, as one can observe from Eq. (6). Further, it is clear from Eq. (9) that the local part of G^{dual} cannot have always-positive imaginary part. However, this does not result in a causality problem: analytical properties of the nonlocal space part G^{dual}_{ij} are similar to that of the G_{ij} for $i \neq j$, whereas the local part of the dual propagator does not enter any diagram.

As the most challenging test of our approximation scheme in the intermediate regime, we performed the calculation for the half-filled square-lattice Hubbard model at sufficiently low temperature $\beta^{-1}=|t|/5$. The value of U was varied from small numbers to a bandwidth $8|t|$. The block scheme of our calculation is shown in Fig. 1. It has good practical convergence: typically, about ten iterations are enough to ensure convergence.

In order to obtain a reference point for a further comparison with the results of our approximation scheme, we performed a direct lattice QMC calculation with the continuous-time QMC code.[30] There are strong antiferromagnetic fluctuations in the system, although true antiferromagnetism is impossible at finite temperature in the 2D system with an isotropic order parameter.[29] Consequently, the increase of U results in the formation of an antiferromagnetic pseudogap.

It was also noticed that a single-site DMFT calculation for this system shows no pseudogap in the density of states, although the data for the local part of the self-energy are reproduced quite well in DMFT. Thus, we concluded that the formation of a pseudogap is entirely related to the nonlocal part of Σ, neglected in DMFT.

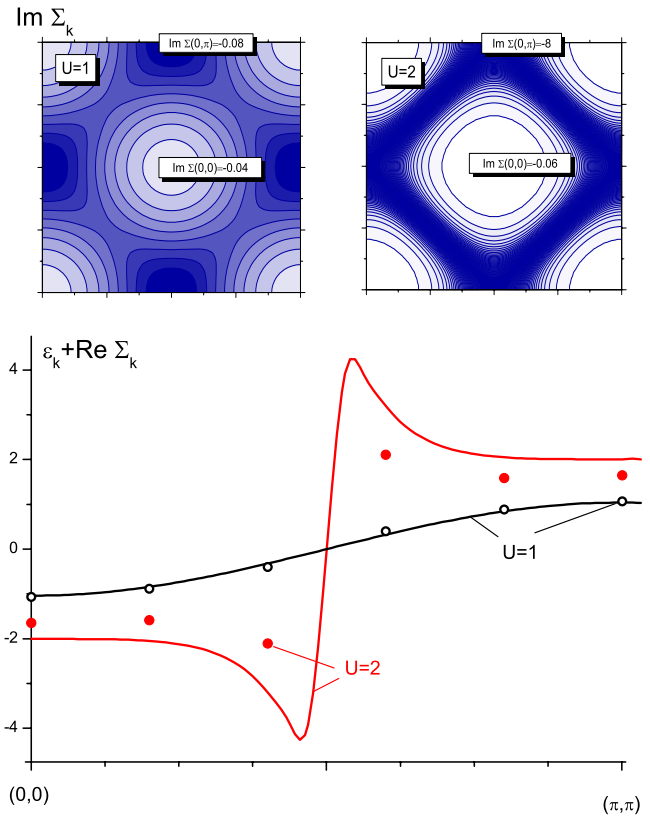

FIG. 2. (Color online) Fermi-energy properties of the half-filled Hubbard model calculated with the leading dual diagram correction b. The calculations have been performed for the bandwidth $8t=2$ at $\beta=20$, for different values of U. Upper panels are contour plots for $\mathrm{Im}\,\Sigma_k$ at the Fermi energy. At $U=1$, $\mathrm{Im}\,\Sigma$ peaks in the four van Hove points, whereas $\mathrm{Im}\,\Sigma(U=1)$ is approximately constant in all points of the Fermi surface. Note also that the change from $U=1$ to $U=2$ leads to a 10^2 increase in $\mathrm{Im}\,\Sigma$. The lower panel shows a graph of the effective dispersion law, $\epsilon_k+\mathrm{Im}\,\Sigma_k$ at Fermi level, plotted along the $(0,0)$-(π,π) direction. The initial "cosine" dispersion law ϵ_k is almost not renormalized at $U=1$. On the contrary, for $U=2$, the curve shows the antiferromagnetic properties. The results of the direct QMC 10×10 lattice simulation are shown with dots and confirm this picture.

We present the results of the dual fermion calculation with only diagram (b) (Fig. 1) taken into account. All other diagrams are smaller both in the strong-coupling and weak-coupling regimes, due to extra vertices or extra lines, respectively. Computational results are illustrated in Fig. 2. The upper panel shows an imaginary part of the self-energy. In the DMFT, this quantity is momentum independent. Our calculations show a very strong **k** dependence, with a maximum near the Fermi surface. At relatively small value $U=1$, the peaks of $\mathrm{Im}\,\Sigma$ are located near the van Hove singularities (left picture), as can be understood from the weak-coupling expansion. On the contrary, for an antiferromagnetic system near the atomic limit, $\mathrm{Im}\,\Sigma_{k,\omega=0}$ would be a simple delta

function peaking at the Fermi surface. For a pseudogap regime at finite β and U, the width of this peak is, of course, finite, but the altitude almost does not depend on the point at the Fermi surface (right picture). The lower panel shows an effective renormalized dispersion law $\epsilon_k + \mathrm{Re}\,\Sigma_{k,\omega=0}$. For the metallic regime, there renormalization is small. For an antiferromagnetic insulator, there would be a pole in $\mathrm{Re}\,\Sigma_{k,\omega=0}$ at the Fermi surface. For the pseudogap regime, fluctuations virtually move this pole from the real-frequency axes, as the curve for $U=2$ shows.

Thus, our scheme continuously interpolate between the two very different regimes. It should be stressed that the quantities under study have very strong k dependence and that it would be very difficult to obtain the result of this kind, for example, in cluster calculations. Whereas for the weak-coupling regime effective schemes to calculate nonlocal self-energy are known, such as FLEX (Ref. 28) or parquet,[16] to our knowledge, there is no alternative scheme yet for the strong-coupling case.

To conclude, we have formulated an effective perturbation theory to calculate the momentum dependence of self-energy starting with single-site DMFT or any local approximations. The vertices of the effective impurity problem play the role of formal small parameters. Due to the transformation to dual fermionic variables, consideration of a few leading diagrams provides a quite satisfactory description of the nonlocal correlation effects in a broad range of parameters, up to the atomic limit. This scheme can be easily generalized to the multiband case to be implemented into realistic electronic structure calculations for strongly correlated systems.

The work was supported by NWO Project No. 047.016.005 and FOM (the Netherlands), DFG Grant No. SFB 668-A3 (Germany), and leading scientific schools program and "Dynasty" Foundation (Russia).

[1] J. Hubbard, Proc. R. Soc. London, Ser. A **276**, 238 (1963).
[2] D. J. Scalapino, Phys. Rep. **251**, 1 (1994); J. Low Temp. Phys. **117**, 179 (1999).
[3] P. W. Anderson, *The Theory of Superconductivity in High-T_c Cuprates* (Princeton University Press, Princeton, NJ, 1997).
[4] T. Moriya, *Spin Fluctuations in Itinerant Electron Magnetism* (Springer, Berlin, 1985).
[5] A. Georges, G. Kotliar, W. Krauth, and M. J. Rozenberg, Rev. Mod. Phys. **68**, 13 (1996).
[6] G. Modugno, F. Ferlaino, R. Heidemann, G. Roati, and M. Inguscio, Phys. Rev. A **68**, 011601(R) (2003); M. Köhl, H. Moritz, T. Stöferle, K. Günter, and T. Esslinger, Phys. Rev. Lett. **94**, 080403 (2005); J. K. Chin, D. E. Miller, Y. Liu, C. Stan, W. Setiawan, C. Sanner, K. Xu, and W. Ketterle, Nature (London) **443**, 961 (2006).
[7] E. Dagotto, Rev. Mod. Phys. **66**, 763 (1994).
[8] R. Blankenbecler, D. J. Scalapino, and R. L. Sugar, Phys. Rev. D **24**, 2278 (1981).
[9] J. E. Hirsch and R. M. Fye, Phys. Rev. Lett. **56**, 2521 (1986).
[10] H. De Raedt and A. Lagendijk, Phys. Rev. Lett. **46**, 77 (1981); H. De Raedt and M. Frick, Phys. Rep. **231**, 107 (1993).
[11] A. C. Hewson, *The Kondo Problem to Heavy Fermions* (Cambridge University Press, Cambridge, England, 1993).
[12] A. I. Lichtenstein, M. I. Katsnelson, and G. Kotliar, Phys. Rev. Lett. **87**, 067205 (2001).
[13] G. D. Mahan, *Many-Particle Physics* (Plenum, New York, 1993).
[14] T. Maier, M. Jarrell, T. Pruschke, and M. Hettler, Rev. Mod. Phys. **77**, 1027 (2005).
[15] A. I. Lichtenstein and M. I. Katsnelson, Phys. Rev. B **62**, R9283 (2000).
[16] V. Yu. Irkhin, A. A. Katanin, and M. I. Katsnelson, Phys. Rev. B **64**, 165107 (2001); Phys. Rev. Lett. **89**, 076401 (2002).
[17] J. Schäfer, M. Hoinkis, E. Rotenberg, P. Blaha, and R. Claessen, Phys. Rev. B **72**, 155115 (2005).
[18] G. Kotliar, S. Y. Savrasov, G. Palsson, and G. Biroli, Phys. Rev. Lett. **87**, 186401 (2001).
[19] M. Potthoff, M. Aichhorn, and C. Dahnken, Phys. Rev. Lett. **91**, 206402 (2003).
[20] V. V. Mazurenko, A. I. Lichtenstein, M. I. Katsnelson, I. Dasgupta, T. Saha-Dasgupta, and V. I. Anisimov, Phys. Rev. B **66**, 081104(R) (2002).
[21] A. I. Poteryaev, A. I. Lichtenstein, and G. Kotliar, Phys. Rev. Lett. **93**, 086401 (2004).
[22] S. Biermann, A. Poteryaev, A. I. Lichtenstein, and A. Georges, Phys. Rev. Lett. **94**, 026404 (2005).
[23] H. Kusunose, J. Phys. Soc. Jpn. **75**, 054713 (2006).
[24] A. Toschi, A. A. Katanin, and K. Held, Phys. Rev. B **75**, 045118 (2007).
[25] Of course, the Bethe-Salpeter equation itself is exact, irrespective of the value of U, up to atomic limit. However, the first step of the procedure produces an approximate vertex Γ, which is insufficient in the case of large U.
[26] J. M. Luttinger and J. C. Ward, Phys. Rev. **118**, 1417 (1960).
[27] G. Baym, Phys. Rev. **127**, 1391 (1962).
[28] N. E. Bickers and D. J. Scalapino, Ann. Phys. (N.Y.) **193**, 206 (1989).
[29] N. D. Mermin and H. Wagner, Phys. Rev. Lett. **17**, 1133 (1966).
[30] A. N. Rubtsov, V. V. Savkin, and A. I. Lichtenstein, Phys. Rev. B **72**, 035122 (2005).